シンにどう影響するか，視床下部副腎皮質系とどうかかわるかは今後の課題である．

今回の結果は薬物治療や手術治療[4)23)～26)]に疑問を抱かせる．特徴的な行動による疲労や心労が病因であれば，治療の要は早期の生活指導に尽きる．まず熱中行動や自己抑制が有害なことを自覚させ，睡眠の確保，仕事量の減少，我慢して頑張らないなど．第2に発散行為や楽しみを充実させることで，個人の自由行動を増やす，スポーツで汗を流す，談笑や楽しい会食，趣味の実践など．生活指導は早期に具体的内容で，徹底して実施される必用があり[4)]，診断基準[27)]の改定と再発予防のガイドライン作成が早急に望まれる．

結　論

1．内リンパ水腫患者群（調査項目により n＝131～209）を対象として，日常の過ごし方 8 項目，行動特性 24 項目，ストレス源 22 項目，気分転換手段 11 項目，身体症状 5 項目のアンケート調査結果を分析し，一般勤労者群（n＝3,410）と比較した．さらに患者群（n＝120～171）でストレスのかかわり，発症や増悪要因をアンケート調査し分析した．

2．患者群は，熱中しやすく徹底的にやる，事前にいろいろ心配する，嫌なことでも我慢し親や上司の期待にそう，イライラしたり怒りやすい，などの行動が勤労者群に比べ著しかった（P＜0.005）．患者群で休息日が少なく（P＜0.0001），汗を流す手段や談笑が不足し，周囲の評価や人間関係に過敏なことが確認された（P＜0.05）．

3．患者群の約7割が発症や増悪にストレスのかかわりを自覚していた．発症や増悪の要因は全世代で多忙，睡眠不足が突出したが，男女間，世代間で違いがみられた．男性は職場の，女性は家庭の関連項目が目立った．20 代は睡眠不足，40 代は職場の対人関係，60 代は家庭トラブルが特徴的であった．

4．疲労を招く行動特性と疲労回復手段の不足が発症や増悪の要因と示唆された．内リンパ水腫は生活習慣病の可能性が強く，仕事量を減らし睡眠時間を増やすこと，快い汗を流す手段や談笑の機会を持つこと，義務的な交友や家庭団らんから離れた個人の自由時間を持つことが，治療に効果的と結論される．

謝　辞

本研究は，厚生労働省特定疾患，前庭機能異常調査研究分科会の平成 14～15 年度の研究活動として行われたものであり，謝意を表します．本研究の症例の一部は，山口大学耳鼻咽喉科，茅ヶ崎中央病院耳鼻咽喉科にご協力いただいたものです．ご協力いただいた山下裕司氏，菅原一真氏，石田克紀氏に謝意を表します．

参考文献

1）渡辺行雄，水越鉄理，中川　肇，他：メニエール病の症例対照調査結果．Equilibrium Res 補 7：1～10，1991.
2）水越鉄理，将積日出男，渡辺行雄：メニエール病の疫学―本邦の調査研究を中心に―．Equilibrium Res 56：219～233，1997.
3）高橋正紘，大賀純一，小田桐恭子，他：内リンパ水腫の聴力変動にみられる規則性．Otology Japan 13：135～140，2003.
4）高橋正紘，大賀純一：メニエール病の生活指導．耳鼻咽喉科診療プラクティス 6．EBM に基づくめまい診断と治療（武田憲昭編）．134～138 頁，文光堂，東京，2001.
5）Takahashi M, Ishida K, Iida M, et al.: Analysis of lifestyle and behavioral characteristics in Meniere's disease patients and a control population. Acta Otolaryngol 121：254～256，2001.
6）高橋正紘：メニエール病―発症・増悪要因を探る―．耳鼻頭頸 74：837～841，2002.
7）山下裕司，下郡博明，綿貫浩一，他：メニエール病とタイプ A 行動特性．耳鼻臨床 90：1209～1213，1997.
8）山下裕司，菅原一真，下郡博明，他：メニエール病患者の行動特性についてーアンケートによるストレスの定量化―．Equilibrium Res 57：428～434，1998.
9）杉山善朗，佐藤　豪：タイプ A 行動．医療・健康心理学（中川米造，宗像恒次編）．63～81 頁，福村出版，東京，1989.
10）宗像恒次：健康と病気の社会，心理，文化背景．最新行動科学からみた健康と病気．1～44 頁，メヂカルフレンド社，東京，1996.
11）宗像恒次：ストレスと対処行動．医療・健康心理学（中川米造，宗像恒次編）．1～21 頁，福村出版，東京，1989.
12）大賀純一，高橋正紘，山下裕司：勤労者 3,400 名における行動特性，ストレス源ならびに身体症状のアンケート調査結果．厚生省特定疾患前庭機能異常調査研究分科会　平成12年度研究報告書，57～60 頁，2001.
13）高橋正紘，大賀純一，小田桐恭子，他：一般勤労者と内リンパ水腫患者のライフスタイル・アンケートの比較．厚生省特定疾患前庭機能異常調査研究分科会　平成10年度研究報告書，77～81 頁，1999.
14）高橋正紘：メニエール病の謎．耳鼻臨床 95：210～211，2002.
15）Hagnebo C, Andersson G and Melin L: Correlates of vertigo attacks in Meniere's disease. Psychother Psychosom 67：311～316，1998.
16）Coker NJ, Coker RR, Jenkins HA, et al.: Psychological profile

of patients with Meniere's disease. Arch Otolaryngol Head Neck Surg **115**：1355～1357, 1989.
17) Martin C, Martin H, Carre J, et al.：Meniere's disease; a psychosomatic disease? Rev Laryngol Otol Rhinol (Bord) **112**：109～111, 1991.
18) Arweiler DJ, Jahnke K and Grosse-Wilde H：Meniere's disease as an autosome dominant hereditary disease. Laryngorhinootologie **74**：512～515, 1995.
19) Imai K and Nakachi K：Personality types, lifestyle, and sensitivity to mental stress in association with NK activity. Int J Hyg Environ Nealth **204**：67～73, 2001.
20) Carrasco GA and Van de Kar LD：Neuroendocrine pharmacology of stress. Eur J Pharmacol **463**：235～272, 2003.
21) Takeda T, Kakigi A and Saito H：Antidiuretic hormone (ADH) and endolymphatic hydrops. Acta Otolayrngol Suppl 519：219～222, 1995.
22) Juhn SK, Li W, Kim JY, et al.：Effect of stress-related hormones on inner ear fluid homeostasis and function. Am J Otol **20**：800～806, 1999.
23) Thorp MA, Shehab ZP, Bance ML, et al.：Does evidence-based medicine exist in the treatment of Meniere's disease? A critical review of the last decade of publications. Clin Otolaryngol **25**：456～460, 2000.
24) Stahle J, Friberg U and Svedberg A：Long-term progression of Meniere's disease. Am J Otol **10**：170～173, 1989.
25) Green JD Jr, Blum DJ and Harner SG：Longitudinal followup of patients with Meniere's disease. Otolaryngol Head Neck Surg **104**：783～788, 1991.
26) Kinney SE, Sandridge SA and Newman CW：Long-term effects of Meniere's disease on hearing and quality of life. Am J Otol **18**：67～73, 1997.
27) 渡辺いさむ：厚生省研究班のメニエール病診断基準について. 耳鼻臨床 **69**：301～303, 1976.

別刷請求先：高橋正紘
〒259-1193 伊勢原市望星台
東海大学医学部耳鼻咽喉科

Acta Otolaryngol 2004; Suppl 553: 6–12

Taylor&Francis
healthsciences

Interferon-γ Expression in the Inner Ear of Rats Following Secondary Immune Reaction in the Endolymphatic Sac

RUBY PAWANKAR, SHUNICHI TOMIYAMA, TETSUO IKEZONO, MANABU NONAKA, KEN JINNOUCHI and TOSHIAKI YAGI

From the Department of Otolaryngology, Nippon Medical School, Tokyo, Japan

Pawankar R, Tomiyama S, Ikezono T, Nonaka M, Jinnouchi K, Yagi T. *Interferon-γ expression in the inner ear of rats following secondary immune reaction in the endolymphatic sac.* Acta Otolaryngol 2004; Suppl 553: 6–12.

Recently, we demonstrated increased intercellular adhesion molecule-1 (ICAM-1) expression in the inner ear of systemically pre-sensitized rats after antigen [keyhole limpet hemocyanin (KLH)] challenge into the endolymphatic sac (ES), in good correlation with the cellular infiltration. Interferon-γ (IFN-γ) is an important cytokine that upregulates the expression of ICAM-1. Here, we report upregulation of IFN-γ expression in the inner ear of systemically pre-sensitized rats after antigen (KLH) challenge into the ES. Immunoreactivity for IFN-γ was detected in the spiral ligament, suprastrial region, spiral modiolar veins, spiral collecting venules, surface membrane of the perilymphatic compartment and perilymphatic space of immunized, but not control, rats. IFN-γ expression was detected at 1.5 h post-challenge, peaked at 6 h and gradually returned to baseline levels after 7 days. Interestingly, the time kinetics of IFN-γ expression were in good correlation with those of ICAM-1. These observations demonstrate that antigen challenge into the ES induces IFN-γ expression, which can then upregulate ICAM-1 expression and induce cell infiltration, suggesting that IFN-γ may play a crucial role in immune-mediated inner ear diseases. *Key words: cellular infiltration, endolymphatic hydrops, inner ear, intercellular adhesion molecule-1, interferon-γ.*

INTRODUCTION

It has been suggested (1) that immune injury of the inner ear may be an important etiology of various inner ear diseases. It has been demonstrated (2) that the inner ear is capable of independently mounting an immune response and that the endolymphatic sac (ES) plays an integral role in the inner ear immune response (3). Recruitment of immunocompetent cells from the systemic circulation into the inner ear is a prerequisite for the development of this immune response. However, the precise mechanisms involved in the recruitment of these immunocompetent cells into the inner ear remain unknown.

Previously, we demonstrated (4–6) that secondary antigen challenge directly into the ES of guinea pigs resulted in fluctuating hearing loss, spontaneous nystagmus, a suppressed caloric response and rapid formation of endolymphatic hydrops. These functional disorders were associated with the infiltration of a large number of immunocompetent cells into the ES. In addition, a small number of cells were detected in the perilymphatic space of the cochlea, probably as a result of migration from the spiral collecting venules. It is well known (7, 8) that adhesion molecules control cellular interactions within the immune system and play a critical role in regulating leukocyte homing. Thus, changes in the expression of adhesion molecules on endothelial cells and circulating leukocytes are clearly important factors in controlling the formation of cellular exudates at sites of inflammation (9). Intercellular adhesion molecule-1 (ICAM-1) is an 80–115-kDa glycoprotein belonging to the Ig super-family and is expressed on the surface of a variety of leukocytes and other cell types (10). We recently demonstrated (11) that ICAM-1 was strongly expressed at various sites in the cochlea after secondary injection of antigen into the ES.

The development of distinct subsets of CD4+ T cells during an immune response, which is distinguished by their ability to produce distinct patterns of cytokines, is well known. Th1 cells produce interferon-γ (IFN-γ) and lymphotoxin, which mediate cell-mediated immune responses but may also be implicated in the immunopathology resulting from organ-specific autoimmune diseases (12–14). IFN-γ is known to suppress the production of Th2-type cytokines and plays an important role in the upregulation of adhesion molecules such as ICAM-1 on endothelial cells, which results in the recruitment of inflammatory cells (15). In the light of the above, the present study was designed to elucidate the mechanisms involved in the recruitment of immunocompetent cells into the inner ear after secondary antigen challenge into the ES, by investigating the expression of IFN-γ in the inner ear after such a challenge, its relation to the expression of ICAM-1 and cell infiltration into the inner ear and the development of endolymphatic hydrops.

Our previous results (11) demonstrated that IFN-γ was expressed in the cochlea of secondary challenged rats, although the challenged antigen was only localized to the ES. In addition, the intensity and time course of IFN-γ expression were in good correlation with those of ICAM-1 expression and cell infiltration into the cochlea, suggesting that IFN-γ may be an

 ISSN 0365-5237

DOI 10.1080/03655230410017580

important cytokine involved in the recruitment of immunocompetent cells in an inner ear immune response.

MATERIAL AND METHODS

Animals

The methods for the induction of endolymphatic hydrops are as previously described (4–6). Briefly, PVG/se rats were systemically immunized with 500 μg of keyhole limpet hemocyanin (KLH)/complete Freund's adjuvant and boosted twice with KLH/incomplete Freund's adjuvant once every 2 weeks until a high serum anti-KLH level was obtained. Two weeks later, under general anesthesia, KLH (30 μg in 1 μl) was directly injected into the ES of the animals via the intradural approach. Animals thus immunized and challenged (with antigen or PBS) were sacrificed at various time points (1.5, 3, 6, 12 and 15 h, 1, 2, 4, 7 and 14 days) by intracardiac perfusion of warm saline followed by periodate–lysine paraformaldehyde (PLP), which also served as a fixative. For each point of termination we used at least six experimental animals. Temporal bones were dissected out and fixed for 3 h in the same fixative, decalcified for 3 weeks in 10% EDTA at 4°C, washed in a graded series of sucrose in PBS (10%, 15% and 20%), embedded in optimal cutting temperature compound, frozen in liquid nitrogen and stored at −80°C until further use. Lymph nodes of systemically immunized rats were removed and processed in the same manner and used as positive controls.

Immunohistochemical analysis for the detection of IFN-γ expression in the inner ear

IFN-γ expression was detected with the mouse anti-rat IFN-γ monoclonal antibody (mAb; BioSource, USA) using the alkaline phosphatase anti-alkaline phosphatase (APAAP) method (Dako APAAP kit; Dako, Carpinteria, CA). Briefly, 5-μm thick serial sections were cut, air-dried, rehydrated in Tris-buffered saline (TBS), pH 7.6, pretreated with 10% normal rabbit serum for 10 min and incubated with the anti-rat IFN-γ mAb for 30 min. Subsequently, the sections were incubated with the rabbit anti-mouse IgG for 30 min and then with the APAAP reagent for 30 min. Between each incubation the sections were rinsed in TBS. The reaction was developed by incubation with the substrate Naphthol AS-MX Fast-Red TR. Finally, the sections were rinsed in distilled water, counterstained with Mayer's hematoxylin and mounted in Dako gel. The lymph nodes of systemically immunized rats were used as positive controls. As a negative control, the primary mAb was substituted by an isotype-matched unrelated mAb (mouse myeloma IgG1; Dako).

Immunohistochemical analysis for the detection of ICAM-1 expression in the inner ear

ICAM-1 expression was detected with the mouse anti-rat ICAM mAb (R & D Systems, Abingdon, UK) using the APAAP method as described above. As a negative control, the primary mAb was substituted by an isotype-matched unrelated mAb (mouse myeloma IgG1; Dako).

Intensity of IFN-γ immunoreactivity in the inner ear of PVG/se rats

The intensity of IFN-γ expression in the inner ear was graded into four degrees of staining intensity as follows: −, no staining; ±, minimal; +, mild; ++, moderate; and +++, marked staining.

Histological analysis for the detection of cell infiltration in the inner ear of PVG/se rats

At the termination of each experiment (5 h, 10–15 h, 1 day and 7 days following secondary KLH challenge into the ES), a total of 24 experimental rats and 10 control rats were sacrificed by intracardiac perfusion with warm saline followed by PLP fixative. Temporal bones were fixed with PLP for a further 3 h, decalcified in 10% buffered EDTA for 3 weeks in a cold room, embedded in paraffin, serially sectioned at a thickness of 5 μm parallel to the modiolus and stained with hematoxylin–eosin for light microscopic examination. The control animals were injected with PBS into the ES. Cellular infiltration into the cochlea was determined as follows: the maximum number of infiltrating cells in any section was taken as the representative number of infiltrated cells for the cochlea. Grading of cell infiltration was performed as follows: Grade 0, no cells; Grade 1, 1–9 cells; Grade 2, 10–19 cells; Grade 3, >20 cells.

RESULTS

IFN-γ immunoreactivity in the inner ear of normal controls and secondary challenged rats

IFN-γ immunoreactivity was distinctly detected with varying degrees of intensity in the inner ear of immunized rats (Table I). Negative controls showed no staining (Fig. 1A and 1B). Almost no immunoreactivity for IFN-γ was detected in the inner ears of PBS-challenged rats at any time point. The distribution of IFN-γ immunoreactivity is described in the following sections.

Table I. *Immunoreactivity of IFN-γ in the inner ear of PVG/se rats following secondary challenge to the ES*

Region	Precise anatomical site	Intensity of IFN-γ expression
Spiral ligament	Suprastrial region	+
	Inferior part	++
Stria vascularis	Marginal cells	−
	Intermediate cells	−
	Basal cells	−
	Endothelial cells	+
Spiral prominence	Epithelial cells	−
	Subepithelial area	+
Organ of Corti	Inner phalangeal cells, border cells, Deiter's cells, Hensen's cells, Claudius cells and Boettcher's cells	±
	Inner hair cells	−
	Outer hair cells	−
Spiral limbus	Interdental cells	−
	Supralimbus	±
	Tectorial membrane	+
Basilar membrane	Epithelial cells	−
	Basilar membrane	±
Reissner's membrane		+
Modiolar region	Modiolar veins and arteries	+++
	Capillaries of spiral ganglion	++
Utricle and Saccule	Epithelial cells	−
	Subepithelial area	+
Crista ampularis	Epithelial cells	−
	Subepithelial area	+
ES		++

The lateral wall of the cochlear duct

The spiral ligament. IFN-γ immunoreactivity was not detected in the spiral ligament of normal control PVG/se rats at baseline. However, moderate levels of IFN-γ immunoreactivity were detected in the suprastrial region and in the inferior part, starting at 1.5 h and peaking at 6 h post-challenge (Table I, Fig. 1C). In the basal turn, IFN-γ immunoreactivity in the suprastrial region persisted for 24 h, whereas it persisted for ≈2 days in the inferior part. In contrast, IFN-γ immunoreactivity in the suprastrial region of the second turn was detectable only until 12 h post-challenge, but that in the inferior part was detectable until 2 days post-challenge (Fig. 1D and 1E).

The stria vascularis. IFN-γ immunoreactivity was not detected either on the surface membrane of marginal cells or in the intermediate or basal cells of normal control rats at baseline or after secondary challenge (Table I).

The spiral prominence and external sulcus. IFN-γ immunoreactivity was not detected in the epithelial cells of the spiral prominence or the root cells of the external sulcus in normal control rats at baseline or after secondary challenge. However, the endothelium of the spiral prominence demonstrated weak immunoreactivity for IFN-γ in the secondary challenged rats at 6 h post-challenge (Table I).

The tympanic wall of the cochlear duct

The organ of Corti. IFN-γ immunoreactivity was not detected in the inner or outer hair cells of normal control rats at baseline or after secondary challenge. However, after secondary challenge, negligible immunoreactivity for IFN-γ was detected in Deiter's cells, Boettcher's cells, inner phalangeal cells, border cells, Hensen's cells and Claudius cells (Table I).

The spiral limbus. Negligible IFN-γ immunoreactivity was detected in the superior part of the spiral limbus and in the supralimbal area but not in the interdental cells of secondary challenged rats at 6 h post-challenge. Weak IFN-γ expression was also detected in the tectorial membrane (Table I). However, immunoreactivity for IFN-γ was not detected in normal control rats at baseline.

Basilar membrane. Epithelial cells exhibited no immunoreactivity for IFN-γ expression. However, the basilar membrane exhibited low levels of IFN-γ immunoreactivity (Table I).

The vestibular wall of the cochlear duct

Reissner's membrane. Negligible IFN-γ immunoreactivity was detected on both surfaces of Reissner's membrane at 12 h post-challenge (Table I).

The modiolar region. The modiolar veins and arteries of the secondary challenged rats demonstrated

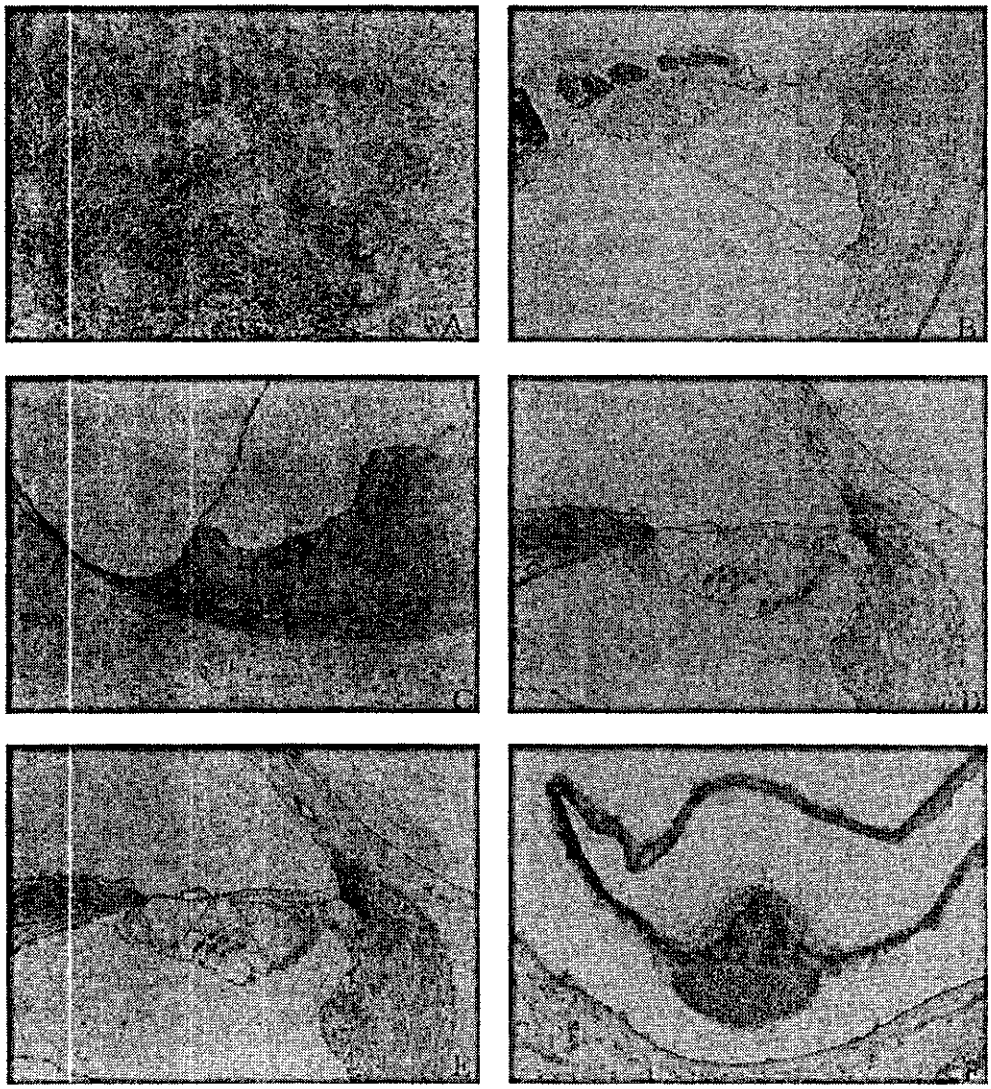

Fig. 1. Immunoreactivity for IFN-γ in the inner ear: (A) negative control (lymph node); (B) negative control (inner ear); (C) IFN-γ expression in the spiral modiolar region at 5 h post-challenge; (D) IFN-γ expression in the suprastrial region of the basal turn at 5 h post-challenge; (E) IFN-γ expression in the second turn at 13 h post-challenge; (F) IFN-γ expression in the lateral crista at 5 h post-challenge.

strong IFN-γ immunoreactivity peaking at Day 1. In addition, moderate IFN-γ immunoreactivity was also detected in the capillaries of the spiral ganglion (Table I).

Utricle and saccule

Although the epithelial cells did not demonstrate any IFN-γ immunoreactivity, moderate IFN-γ immunoreactivity was detected in the subepithelial region of secondary challenged rats (Table I).

Crista ampularis

As observed in the utricle and saccule, epithelial cells of the crista ampularis did not demonstrate any IFN-γ immunoreactivity, but IFN-γ immunoreactivity was detected in the subepithelial region of secondary challenged rats (Table I, Fig. 1F). Immunoreactivity for IFN-γ was not detected in normal control rats at baseline.

ES

Increased levels of immunoreactivity for IFN-γ were detected in the perisaccular region of the ES (Table I).

Time kinetics of IFN-γ and ICAM-1 immunoreactivity in the inner ear of secondary PBS/KLH-challenged PVG/se rats

Assessment of the time kinetics of IFN-γ expression in the inner ear of normal PVG/se rats revealed no baseline IFN-γ expression. IFN-γ immunoreactivity was detected as early as 1.5 h post-challenge, peaked at 5–6 h and plateaued at 13 h. Control rats showed

almost no IFN-γ expression at various survival times (Fig. 2). Assessment of the time course of ICAM-1 expression in the inner ear of PVG/se rats revealed minimal or no baseline ICAM-1 expression. ICAM-1 immunoreactivity was induced at 6 h after antigen challenge, reached a peak at 13 h and was maintained at those levels until Day 1, after which it gradually returned almost to baseline levels at 2 weeks (Fig. 2). In contrast, IFN-γ expression was detected as early as 1.5 h, peaked at 6 h and was undetectable by 1 week after antigen challenge (Fig. 3).

Time kinetics of cell infiltration in the cochlea of PVG/se rats

Cell infiltration (Grade 1) was detected as early as 6 h in the basal and second turns, increased at 12 h (Grade 2) and peaked at Day 1 (Grade 3) (Fig. 4). At Day 7 only a few cells were detected. The time kinetics of cell infiltration in the basal and second turns were almost the same. Control animals did not demonstrate any cell infiltration into the cochlea at any point of termination.

Comparison of cell infiltration in the scala tympani and scala vestibuli

No difference was noted in cell infiltration at 6 and 12 h. However, at Day 1, cell infiltration was significantly greater in the scala tympani than the scala vestibuli (Fig. 5).

DISCUSSION

An immunological etiology for Ménière's disease has been proposed for a long time (1, 3–5). The ES is the only immunoprivileged site in the inner ear with a resident population of immunocompetent cells as well as a fenestrated vascular system (17). Gloddek and Arnold (18) demonstrated the expression of adhesion molecules in lymphocytes infiltrating the lumen of the ES in a guinea pig model of autoimmune labyrinthitis, and proposed that the ES is the central immunological

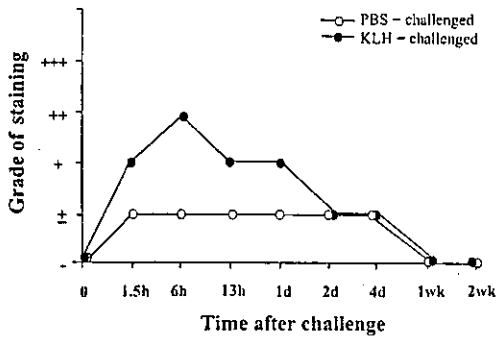

Fig. 2. Time kinetics of IFN-γ expression in the inner ear after ES challenge with PBS or KLH.

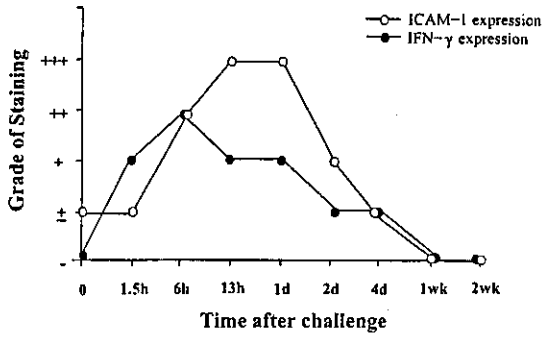

Fig. 3. Time kinetics of IFN-γ and ICAM-1 expression in the inner ear.

control organ of the inner ear and a primary place for antigen processing.

Tomiyama (4) previously demonstrated the occurrence of endolymphatic hydrops in guinea pigs following secondary antigen challenge to the ES. It was also demonstrated that, in addition to infiltration of immunocompetent cells into the perisaccular space and lumen of the ES, a smaller number of inflammatory cells infiltrated into the perilymphatic space of the cochlea and vestibule. As the migration of immunocompetent cells into the perilymphatic space of the cochlea occurs through the spiral collecting venules and vessels of the spiral ligament in the cochlea, we recently investigated the precise mechanisms by which these vessels in the cochlea function as an afferent limb of the immune response in the inner ear. ICAM-1 is an adhesion molecule predominantly expressed in human endothelial vessels (HEVs) in humans, mice and rats and is primarily involved in the interaction between leukocytes and endothelial cells (19). In this context, our recent observations (11) that secondary antigen challenge into the ES of pre-immunized animals resulted in the induction of an immune response in the inner ear characterized by increased expression of ICAM-1, cellular infiltration and development of endolymphatic hydrops emphasizes the role of the ES as the central immunological organ of the inner ear and suggests that ICAM-1 may play a crucial

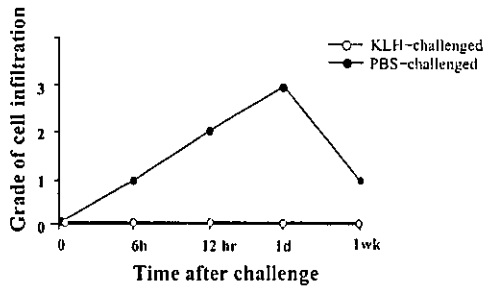

Fig. 4. Time kinetics of cell infiltration in the inner ear of PVG/se rats.

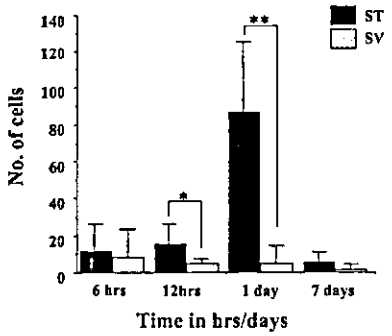

Fig. 5. Comparison of cell infiltration in the scala tympani (ST) and scala vestibuli (SV) of KLH-challenged PVG/se rats.

role in the pathogenesis of immune-mediated inner ear diseases.

IFN-γ is a Th1-type cytokine and one of the potent cytokines known to upregulate the expression of ICAM-1 (15). Therefore, in the present study, we studied the distribution and time kinetics of IFN-γ expression in the inner ear of rats following inoculation of antigen into the ES. Our results demonstrated strong immunoreactivity for IFN-γ in the spiral ligament, suprastrial region, spiral prominence, spiral modiolar veins, spiral collecting venules, the surface membrane of the perilymphatic compartment in the cochlea, the perilymphatic space beneath the vestibular sensory epithelial cells and the endolymphatic sac of immunized rats, but no immunoreactivity for IFN-γ in normal and control rats. In contrast, IFN-γ immunoreactivity was not detected in the stria vascularis or in the outer and inner hair cells, vestibular sensory epithelial cells, transitional cells or dark cells. In this context it is of interest that immunoreactivity for the KLH antigen was detected only in the ES, and not in the cochlea or vestibule of immunized PVG/se rats (11).

Estimation of the time course of IFN-γ immunoreactivity demonstrated the detection of IFN-γ immunoreactivity as early as 1.5 h after immunization. Maximum IFN-γ immunoreactivity occurred at 6 h post-challenge, was reduced by Day 2 and reached baseline levels by Day 7. This was of interest as ICAM-1 immunoreactivity could be detected at 6 h, reaching a maximum at 10–15 h. Furthermore, the strong immunoreactivity of ICAM-1 in the spiral collecting venules and the suprastrial areas of the inferior area of the spiral ligament occurred concomitantly at 12 h with the infiltration of immunocompetent cells into the perisaccular space. This cellular infiltrate comprised predominantly leukocytes and macrophages and was rapidly reduced by Day 7. These close relations between the immunoreactivity for IFN-γ (6 h) and the onset of ICAM-1 expression (13 h), and between the peak of ICAM-1 expression (13 h) and the onset of cellular infiltration (6–12 h) in secondary challenged animals strongly suggests that IFN-γ may upregulate ICAM-1 expression, which in turn may be critical to the recruitment of immunocompetent cells into the inner ear.

Previous studies have demonstrated diffuse dissemination of Ig, complement (20) and myeloperoxidase (21) in the perilymphatic tissue of the vestibule and cochlea following secondary challenge to the ES, suggesting the same diffusion of inflammatory cytokines to the vestibule and cochlea. As we recently demonstrated (11) that the injected antigen KLH was detected only in the ES and not in the cochlea and vestibule, enhancement of IFN-γ expression in the inner ear may occur in response to an immunological stimulus from an immune reaction initiated in the ES resulting in the upregulation of ICAM-1 expression and the infiltration of immunocompetent cells into the posterior spiral modiolar veins and the venules surrounding the ES. This may contribute to the formation of endolymphatic hydrops, probably by increasing the vascular permeability of the vessels in the spiral ligament and suprastrial area and altering the function of the ES.

This study demonstrates for the first time that secondary antigen challenge into the ES of immunized animals results in the induction of IFN-γ locally in the inner ear. The distribution, intensity and time course of the IFN-γ expression were in good correlation with the expression of ICAM-1, suggesting that IFN-γ may play a crucial role in the inner ear immune response via the upregulation of ICAM-1 and the subsequent influx of immunocompetent cells.

REFERENCES

1. Duke WW. Meniere's disease syndrome caused by allergy. JAMA 1923; 81: 2179–81.
2. Harris JP. Immunology of the inner ear: response of the inner ear to antigen challenge. Otolaryngol Head Neck Surg 1983; 91: 17–23.
3. Tomiyama S, Harris JP. The endolymphatic sac: its importance in the inner ear immune responses. Laryngoscope 1986; 96: 685–91.
4. Tomiyama S. Development of endolymphatic hydrops following immune response in the endolymphatic sac of the guinea pig. Acta Otolaryngol (Stockh) 1992; 112: 470–8.
5. Tomiyama S, Nonaka M, Gotoh Y, Ikezono T, Yagi T. Immunological approach to Meniere's disease: vestibular immune injury following immune reaction of the endolymphatic sac. ORL J Otorhinolaryngol Relat Spec 1994; 56: 11–8.
6. Tomiyama S, Kinoshita T, Jinnouchi K, Ikezono T, Gotoh Y, Pawankar R, et al. Fluctuating hearing loss

following immune reaction in the endolymphatic sac. ORL J Otorhinolaryngol Relat Spec 1995; 57: 122–8.
7. Yagita H, Okumura K. The role of adhesion molecules in triggering effector mechanisms. In: Nariuchi H, Okada H, Okumura K, Takatsuki K, Yodoi J, editors. Molecular basis of immune responses. Tokyo: Academic Press; 1993. p. 59–70.
8. Sreeter PR, Berg EL, Bich Tien NR, Bargatse RF, Butcher EC. A tissue specific endothelial cell molecule involved in lymphocyte homing. Nature 1988; 331: 41–6.
9. Dustin ML, Singer KH, Tuck DT, Springer TA. Adhesion of T lymphoblasts to epidermal keratinocytes is regulated by interferon-gamma and is mediated by intercellular adhesion molecule-1 (ICAM-1). J Exp Med 1988; 167: 1323–40.
10. Rothlin R, Dustin ML, Marlin SD, Springer TA. A human intercellular adhesion molecule (ICAM-1) distinct from LFA-1. J Immunol 1986; 137: 1270–4.
11. Pawankar R, Tomiyama S, Jinnouchi K, Ikezono T, Nonaka M, Yagi T. ICAM-1 expression in the inner ear following secondary immune reaction in the endolymphatic sac. Acta Otolaryngol (Stockh) 1998; 539: 6–11.
12. Mossmann TR, Cherwinski H, Bond MW, Giedlin MA, Coffman RL. Two types of murine helper T cell clone. I. Definition according to profiles of lymphokine activities and secreted proteins. J Immunol 1986; 136: 2348–57.
13. Mossmann TR, Coffman RL. Heterogeneity of cytokine secretion patterns and function of helper T cells. Adv Immunol 1989; 46: 111–47.
14. Fowell D, McKnight AJ, Powrie F, Dyke R, Mason D. Subsets of CD4+ T cells and their roles in the induction and prevention of autoimmunity. Immunol Rev 1991; 123: 37–64.
15. Dustin ML, Rothlein BR, Bhan AK, Dinarello CA, Springer TA. Induction by IL-1 and interferon-γ: tissue distribution, biochemistry, and function of a natural adherence molecule (ICAM-1). J Immunol 1986; 137: 245–54.
16. Dustin ML, Stauton DE, Springer TA. Supergene families in the immune system. Immunol Today 1988; 9: 213–5.
17. Rask-Andersen H, Stahle J. Immunodefense of the inner ear. Lymphocyte-macrophage interaction in the endolymphatic sac. Acta Otolaryngol (Stockh) 1980; 89: 283–4.
18. Gloddek B, Arnold W. Role of adhesion molecules for immunological defense of the inner ear. ORL J Otorhinolaryngol Relat Spec 1995; 57: 10–4.
19. Smith CW, Marlin SD, Rothlein R, Toman C, Anderson DC. Cooperative interactions of LFA-1 and Mac-1 with ICAM-1 in facilitating adherence and transendothelial migration of human neutrophils in vitro. J Clin Invest 1989; 83: 2008–13.
20. Takahashi M, Tomiyama S. Immunohistochemical study of endolymphatic hydrops due to secondary endolymphatic sac immune response. J Otolaryngol (Jpn) 1990; 93: 1372–8.
21. Kinoshita T, Tomiyama S. Free radicals in secondary immune response in guinea pigs. J Otolaryngol (Jpn) 1994; 97: 1608–12.

Address for correspondence:
Ruby Pawankar, MD, PhD
Department of Otolaryngology
Nippon Medical School
1-1-5, Sendagi, Bunkyo-ku
Tokyo 113-8603
Japan
Tel.: +81 3 3822 2131
Fax: +81 3 5685 0830
E-mail: Pawankar_Ruby/ent@nms.ac.jp

Available online at www.sciencedirect.com
SCIENCE DIRECT®
Biochemical and Biophysical Research Communications 314 (2004) 440–446
BBRC
www.elsevier.com/locate/ybbrc

Identification of a novel Cochlin isoform in the perilymph: insights to Cochlin function and the pathogenesis of DFNA9☆

Tetsuo Ikezono,[a,*] Susumu Shindo,[a] Lishu Li,[a] Akira Omori,[b] Sachiyo Ichinose,[b] Atsushi Watanabe,[c] Toshimitsu Kobayashi,[d] Ruby Pawankar,[a] and Toshiaki Yagi[a]

[a] *Department of Otorhinolaryngology, Nippon Medical School, Tokyo, Japan*
[b] *Mitsubishi Kagaku Institute of Life Sciences (MITILS), Tokyo, Japan*
[c] *Department of Biochemistry and Molecular Biology, Nippon Medical School, Tokyo, Japan*
[d] *Department of Otorhinolaryngology, Tohoku University Graduate School of Medicine, Sendai, Japan*

Received 5 December 2003

Abstract

The *COCH* gene mutated in DFNA9, an autosomal dominant hereditary sensorineural hearing loss and vestibular disorder, encodes Cochlin. Previously, we reported three bovine Cochlin isoforms, p63s, p44s, and p40s, which exhibit significant molecular heterogeneity in vivo. Here we have characterized Cochlin isoforms by generating four isoform-specific anti-Cochlin antibodies. The same three Cochlin isoforms, p63s, p44s, and p40s, were detected in human and cow inner ear tissue; however, p44s and p40s were not detected in perilymph. We identified a novel short 16 kDa isoform in human perilymph and a 18–23 kDa isoform in cow perilymph, named Cochlin-tomoprotein (CTP), corresponding to the N-terminus of full-length Cochlin (p63s) and the LCCL domain. Notably, CTP contains all of the known mutation sites associated with DFNA9. The pathogenesis of DFNA9 is not fully clarified as yet, and this novel perilymph-associated CTP isoform might provide mechanistic clues to how mutations in the *COCH* gene damage the inner ear function.

Keywords: Hereditary hearing impairment; DFNA9; *COCH* gene; Cochlin; Human; Inner ear; Isoform; CTP

Mutations in the *COCH* gene have been shown to correlate with DFNA9, an autosomal dominant non-syndromic hearing disorder that causes sensorineural deafness and vertigo [1–7]. We previously performed a proteomic analysis of bovine inner ear proteins to characterize gene products associated with deafness [8]. Our results showed that the protein product of the bovine *Coch* gene [5], Cochlin, constitutes 70% of inner ear protein and is composed of 16 isoforms that are heterogeneous in charge and size. Cochlin isoforms can be classified into three groups, p63s, p44s, and p40s, according to their molecular weight. Analysis of the *COCH* gene in families afflicted with DFNA9 has identified six different single amino-acid mutations, which all converge in the LCCL (Limulus factor C, Cochlin, and late gestation protein Lgl1) domain [9], the only region that shows alterations [10]. Protein sequencing and structure analysis of Cochlin isoforms showed that the mutations influence only the full-length isoform of Cochlin (p63s), and not the processed Cochlin isoforms (p44s and p40s), which do not contain the LCCL domain [8]. What happens to the LCCL domain once it is cleaved from full-length Cochlin is an open issue.

Here, we have generated isoform-specific antibodies that recognize three distinct domains in Cochlin to confirm our previous results and to characterize further the expression and structure of Cochlin isoforms. Using these antibodies, we have analyzed human and bovine inner ear proteins, as well as perilymph proteins, by 1D and 2D Western blot analysis. We have identified a

☆ *Abbreviations:* p63s (plural), isoform p63-1 to p63-8; p44s, isoform p44-1 to p44-5; p40s, isoform p40-1 to p40-3 [8]; 1D-GE, one-dimensional gel electrophoresis; 2D-GE, two-dimensional gel electrophoresis.

* Corresponding author. Fax: +81-3-5685-0830.
E-mail address: tikezono@nms.ac.jp (T. Ikezono).

0006-291X/$ - see front matter © 2003 Elsevier Inc. All rights reserved.
doi:10.1016/j.bbrc.2003.12.106

novel Cochlin isoform in the perilymph that is not present in the inner ear tissue. This shortened isoform, which we designate Cochlin-tomoprotein (CTP), is present in both human and cow as a 16 and a 18–23 kDa protein, respectively, by SDS–PAGE. Our results on the formation and processing of these isoforms in the inner ear will be central to a better understanding of Cochlin function and its role in the pathophysiology of DFNA9.

Materials and methods

Peptide synthesis, immunization, and antibody purification. Using the amino acid sequence of the bovine Cochlin isoforms (for peptides #1, 3, and 4) [8], and that of the human protein deduced from the corresponding gene sequence (for peptide #2), we designed antigenic peptides with the Epitope Advisor program (Fujitsu Kyushu System Engineering) in order to generate isoform-specific antibodies (Figs. 1A and B and Table 1). Peptide #1, which was used to generate "anti-LCCL-N," was an 18-mer (TRGLDIRKEKADVLCPGG) corresponding to residues 36–49 in the N-terminal region of the LCCL domain of full-length Cochlin. Peptide #2, which was used to generate "anti-LCCL-C," was a 14-mer (LSRWSASFTVTKGK) corresponding to residues 114–127 in the LCCL domain; this region is not present in the p44 isoform. Peptide #3, which was used to generate "anti-ivd1," was a 15-mer (AVSTAHPATGKRLKK) corresponding to residues 137–151 in the region between the LCCL domain and the vWF-A1 domain; this region is present in p44s but not in p40s. Peptide #4, which was used to generate "anti-vWF-A1," was a 19-mer (KADIAFLIDGSFNIGQRRF) corresponding to residues 163–181 in the vWF-A1 domain; this sequence is present in all three Cochlin isoforms.

As shown in Table 1, peptides #1 and #4 were completely, and #3 was 93% homologous, with sequences in the human, bovine, and mouse proteins, as deduced from the sequence of the corresponding genes and the sequence of bovine Cochlin [8]. Peptide #2 was 93% homologous with sequences in the mouse protein, as deduced from the sequence of the corresponding gene [11].

We added cysteine residues to the C-termini of peptides #1, #2, and #3 and to the N-terminus of peptide #4 to permit coupling of the peptides to KLH as a carrier protein for immunization. Rabbits were immunized by repeated subcutaneous injections of the KLH-coupled peptides emulsified in incomplete Freund's adjuvant on days 1, 14, 28, and 42. The serum was purified by a protein A column, followed by peptide-affinity chromatography. The specificity of the antibodies for the corresponding antigenic peptides was confirmed by dot blot analysis and a peptide absorption test (data not shown).

Sample preparation. Bovine temporal bones were purchased from a slaughterhouse and guinea-pig temporal bones were removed under deep anesthesia. We first approached the middle ear via the external auditory canal and removed the stapes, and then carefully sucked out the perilymph with a small pipet. By this maneuver, we could minimize contamination from the labyrinthine tissues into the perilymph. Next, we approached the inner ear via the internal auditory canal and dissected the cochlear and vestibular membranous labyrinthine tissues

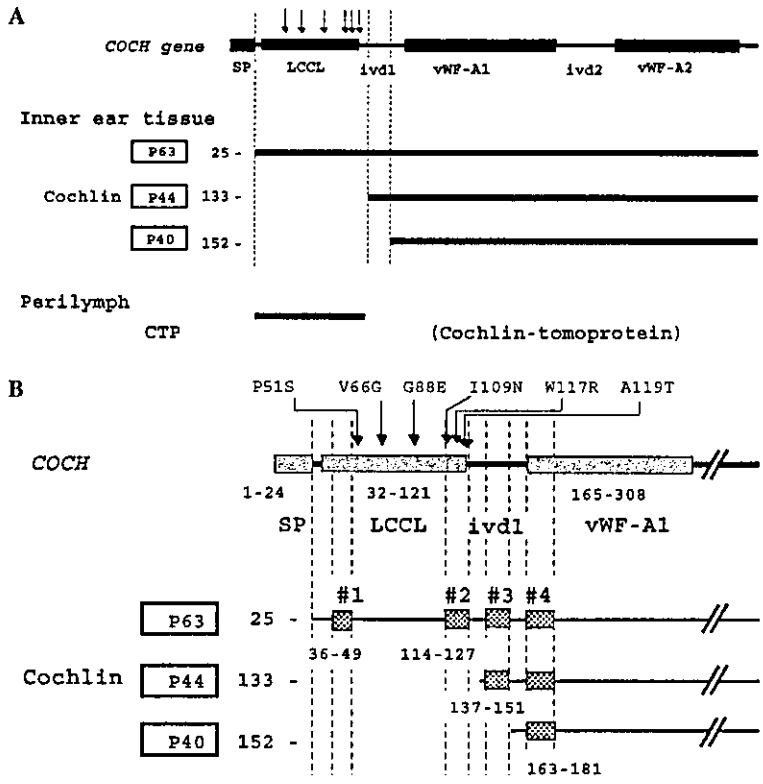

Fig. 1. (A) Representation of the *COCH* gene and Cochlin protein. The top line denotes the deduced amino acid sequence of human *COCH*, showing the positions of the signal peptide (SP), the Limulus factor C, Cochlin and the late gestation lung protein Lgl1 domain (LCCL), the intervening domains 1 and 2 (ivd1,2), and the von Willebrand factor type A like domains 1 and 2 (vWF-A1, vWF-A2). Vertical arrows indicate mutation sites in DFNA9. The middle lines depict bovine Cochlin isoforms, p63s, p44s, and p40s, expressed in inner ear tissue. The numbers of the N-terminal amino acid of each isoform are indicated. The bottom line depicts the Cochlin-tomoprotein (CTP) isoform expressed in the perilymph. (B) Enlargement of the N-terminal region shown in (A). Dashed bars indicate the location of antigenic peptides 1–4. Vertical dashed lines represent the alignment of peptides 1–4 with the amino acid sequence deduced from human *COCH* cDNA and bovine Cochlin.

Table 1
Antigenic peptide design

Isoform		N-terminus position of each isoform in full-length hCOCH	AA sequence	Antigenic peptide	Antigen sequence identity
p63s	human	25-	EGAAPIAITCFTRGLDIRKEKADVLCPGGCPLEEFS	36–49 (#1)	—
	bovine		---V--P--*S----------*---unknown		100
	mouse		---V--PV----------S-----		100
p63s	human	§	YSSVDANGIQSQMLSRWSASFTVIKGKSST	114–127 (#2)	—
	bovine		unknown		
	mouse		----------A--------		93
p44s	human	133-	ATGQAVSTAHPPTGKRLKKTPEKKTGNKD	137–151 (#3)	—
	bovine		----------A----------		93
	mouse		---R--------S----------		93
p40s	human	152-	TPEKKTGNKDCKADIAFLIDGSFNIGQRRFNLQKNFV	163–181 (#4)	—
	bovine		----------*----------unknown		100
	mouse		----------		100

Comparison of the N-terminal amino acid (AA) sequences of the bovine Cochlin isoforms with those deduced from the human *COCH* and mouse *Coch* cDNAs [8]. The N-terminal position of each isoform in full-length human Cochlin is shown in the first column. The sequence identity between human Cochlin and bovine or mouse Cochlin is given. Underlining indicates the sequence of the antigenic peptide used to raise antibodies. *, not determined (cysteine residues cannot be determined definitely by the Edman degradation method); –, the same residue as in human Cochlin. §, human Cochlin amino acids 101–130. § human sequence 101–130.

from bovine temporal bones. We collected human membranous labyrinthine tissues from the posterior and lateral semicircular canals during surgery performed to remove an acoustic neuroma by a translabyrinthine approach. We obtained samples of human perilymph by collecting leakage from the oval window during small fenestra stapedectomy for otosclerosis surgery. Patients gave full informed consent for the use of the surgical specimens. Samples were frozen and stored at −80 °C until use.

One-dimensional gel electrophoresis and Western blot analysis. We prepared a solubilization mixture containing 0.5% SDS and protease inhibitors (Complete mini EDTA(−), Boehringer–Mannheim, Mannheim, Germany) in 10 ml of phosphate-buffered saline (PBS). We homogenized 180 mg of inner ear tissue in 1 ml of solubilization mixture using a mortar and pestle. The homogenate was centrifuged at 1000g for 15 min and the supernatant was used for SDS–PAGE as follows.

Either 0.5 μl of the homogenates prepared from human or bovine inner ear, or 2 μl of perilymph, was diluted with 0.188 M Tris buffer to a total volume of 10 μl and then mixed with 5 μl sample buffer (0.188 M Tris buffer, 2.39 mM SDS, 30% glycerol, and 15% of 2-mercaptoethanol). The samples were heated to 98 °C for 5 min and then loaded into each lane of the gel. Electrophoresis was performed using gels with 3% stacking and either 10% or 15% separating polyacrylamide (ReadyGelJ, Bio-Rad) in the Mini Protean II cell (Bio-Rad) in running buffer (25 mM Tris, 192 mM glycine, and 1 g/L SDS, pH 8.3) at 27 mA for 1 h.

The separated proteins were electrophoretically transferred onto a 0.45 μm nitrocellulose membrane (Bio-Rad) in transfer buffer (25 mM Tris, 192 mM glycine, and 20% v/v methanol, pH 8.3) at 100 V for 90 min. Proteins on the membrane were detected by staining with 3% Ponceau S in 3% sulfosalicylic acid.

Two-dimensional gel electrophoresis and Western blot analysis. Two-dimensional gel electrophoresis (2D-GE) was performed according to our previous report [8]. In brief, first dimension electrophoresis was done by a MultiphorII electrofocusing apparatus (Amersham Pharmacia Biotech). The perilymph was mixed with 20 volumes of solubilization mixture containing 7 M urea, 2 M thiourea, 2% Triton X-100, 1% Pharmalyte, 100 mM dithiothreitol (DTT), and antiprotease mixture (Complete mini EDTA(−), Boehringer-Mannheim, Mannheim, Germany). To detect the target protein (CTP) clearly, we loaded 20 μl of perilymph for Western blot analysis and 15 μl for gels was stained with silver (Silver Stain II, Daiich Pure Chemicals, Tokyo, Japan).

The electrofocusing steps were as follows: 300 V for 60 s, followed by a gradient increase from 300 to 3500 V over 90 min, and then a constant voltage of 3500 V for 18 h. Second dimension electrophoresis was performed using 3% stacking and 15% separating polyacrylamide gels (22 × 20 cm with 1 mm thickness) containing 0.1% SDS in running buffer (25 mM Tris base, 192 mM glycine, and 0.1% SDS) at 35 mA for 5 h. Gels were blotted onto a PVDF membrane and the area of the blot containing the target protein was cut out and subjected to immunodetection. The isoelectric point (pH), relative molecular weight (kDa) of each feature were calculated by the ImageMaster system formally calibrated with respect to two-dimensional size marker, 2D SDS-PAGE standards (Bio-Rad).

Immunodetection. Membranes were blocked overnight at 4 °C in 5% skim milk and 0.2% polyoxyethylenesorbitan (Tween 20) dissolved in PBS (pH 7.4). Membranes were then incubated in PBS containing 1% skim milk and 0.1% Tween 20 for 2 h at room temperature with the primary antibody diluted 1:2000 for the anti-vWF-A1 antibody, and 1:1000 for the anti-LCCL-N, anti-LCCL-C, and anti-ivd1 antibodies. After washing with 0.1% Tween 20 in PBS, membranes were incubated for 1 h at room temperature with horse radish peroxidase-labeled goat anti-rabbit IgG diluted 1:1000 in the same buffer used for the primary antibody reaction. They were washed again and developed with 0.5 mg/ml DAB (3,3′-diaminobenzidine) in 50 mM Tris buffer (pH 7.6) containing 0.03% hydrogen peroxide or a chemiluminescence reaction kit (ECL, Amersham). To strip the antibodies from the membranes, the membranes were incubated at 68 °C for 30 min in stripping buffer (2% SDS,100 mM of 2-mercaptoethanol, and 62.5 mM Tris-HCl, pH 6.8) and then washed with 0.1% Tween 20 in PBS. The membranes were then probed with a second antibody.

Results

1D-GE and Western blot analysis of inner ear tissue

As shown in Fig. 2, the rabbit polyclonal anti-LCCL-N (lane 1) and anti-LCCL-C (lane 2) antibodies,

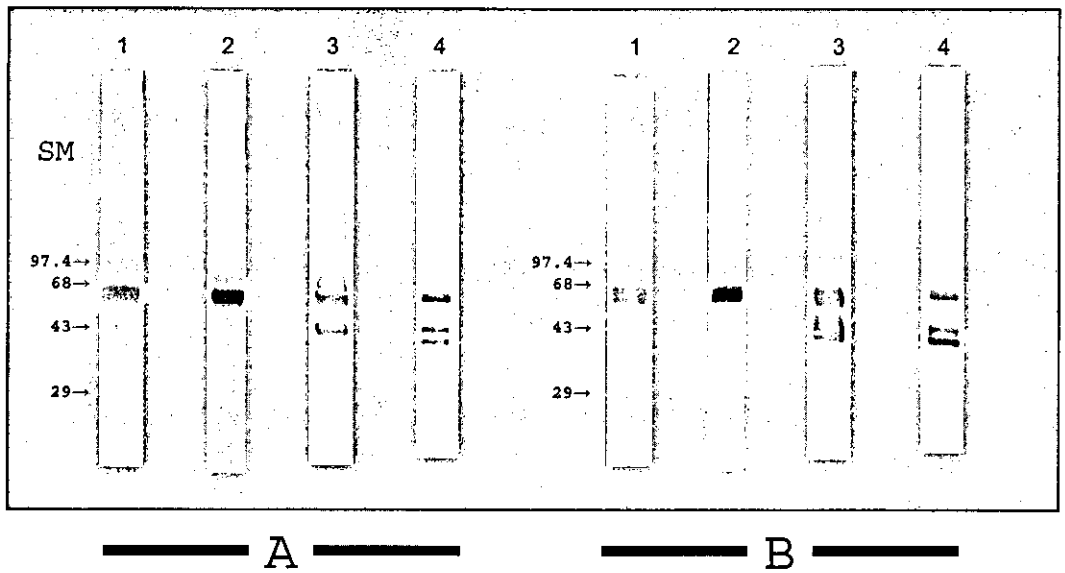

Fig. 2. One-dimensional gel electrophoresis (1D-GE) Western blot analysis of inner ear proteins from human (A) and cow (B) using a 10% separating gel. The anti-LCCL-N (lane 1) and anti-LCCL-C (lane 2) antibodies detected isoform p63s; the anti-ivd1 antibody (lane 3) detected isoforms p63s and p44s; and the anti-vWF-A1 antibody (lane 4) detected isoforms p63s, p44s, and p40s. Proteins were visualized by DAB.

coupled with DAB development, detected a predominant protein of 63 kDa in human (Fig. 2A) and bovine (Fig. 2B) inner ear tissue. The anti-ivd1 antibody reacted with two predominant proteins of 63 and 44 kDa in both types of tissues (lane 3). This antibody also reacted with protein fragments resulting from the degradation of the 63 and 44 kDa proteins. The anti-vWF-A1 antibody detected three distinct proteins in inner ear tissue of 63, 44, and 40 kDa in each lane (lane 4). There were no marked differences in the size and quantity of the proteins detected with these antibodies between human and bovine inner ear tissue.

1D-GE and Western blot analysis of perilymph

In human perilymph (Fig. 3A), the anti-LCCL-N (lane 1) and anti-LCCL-C (lane 2) antibodies, coupled with chemiluminescence, detected a predominant protein of 16 kDa and also reacted with a protein of 60–63 kDa. The anti-ivd1 and anti-vWF-A1 antibodies reacted with protein of 63 kDa (lanes 3 and 4). None of the four antibodies detected proteins of 44–40 kDa, indicating that the p44 and p40 isoforms are not present in human perilymph.

In bovine perilymph (Fig. 3B), the anti-LCCL-N (lane 1) and anti-LCCL-C (lane 2) antibodies detected

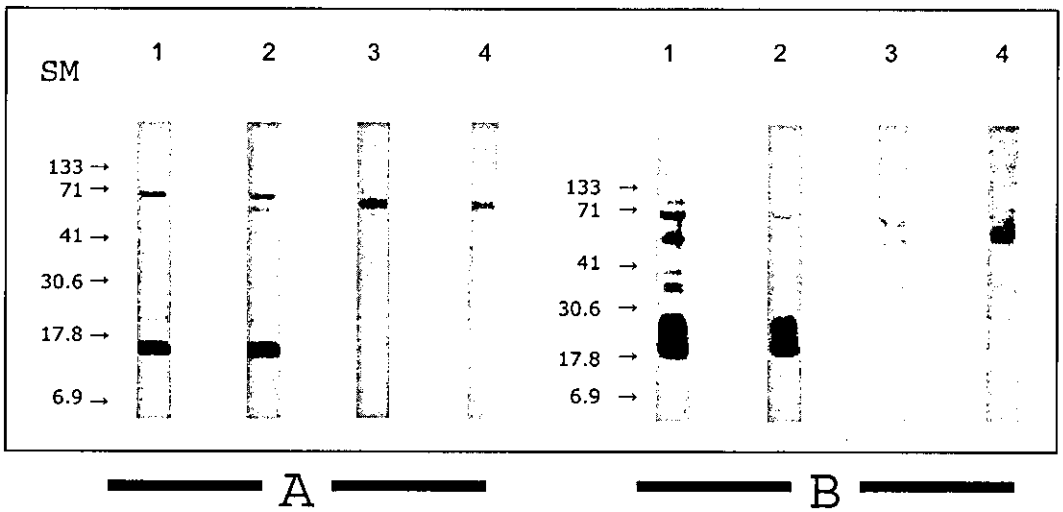

Fig. 3. In human perilymph (A), the anti-LCCL-N (lane 1) and anti-LCCL-C (lane 2) antibodies reacted with CTP (16 kDa) and also with a protein of 60–63 kDa. The anti-ivd1 and anti-vWF-A1 antibodies reacted with a protein of 63 kDa (lanes 3 and 4). None of the four antibodies detected proteins of 44–40 kDa. In bovine perilymph (B), anti-LCCL-N (lane 1) and anti-LCCL-C (lane 2) antibodies detected CTP (18–23 kDa), as well as proteins of 63 kDa. The anti-ivd1 (lane 3) and anti-vWF-A1 (lane 4) antibodies detected proteins of 50–60 kDa. As in human perilymph, none of the antibodies detected the p40 or p44 isoforms. Proteins were visualized by chemiluminescence.

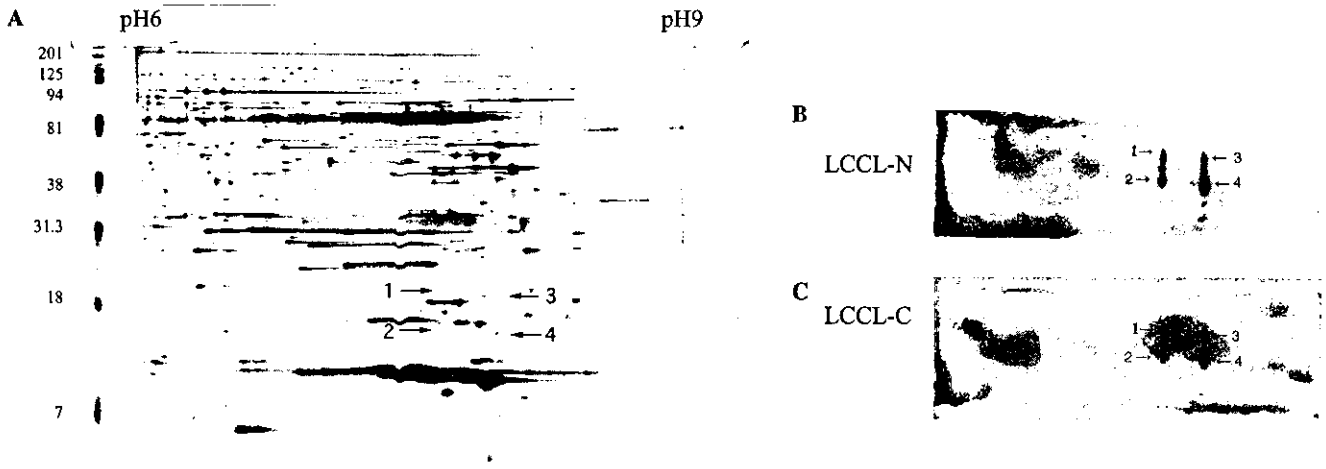

Fig. 4. 2D-GE and Western blot analysis of bovine perilymph. To detect the target proteins clearly, pH6-9 electrofocusing was performed using 20 μl of the perilymph for western blot analysis and 15 μl for the gels stained with silver. (A) Representative 2D-GE gel. Arrows: 1, CTP(7.7), MW 23.1 kDa; 2, CTP(7.7), MW 18.8 kDa; 3, CTP(7.9), MW 22 kDa; and 4, CTP(7.9), MW 17.7 kDa. (B) The blotted membrane was probed with the anti-LCCL-N antibody and the proteins were visualized by chemiluminescence. (C) The membrane was stripped and re-probed with the anti-LCCL-C antibody. These two antibodies detected the same two lines of proteins, CTP(7.7) and CTP(7.9), each composed of protein spots with different molecular weights. Arrows show the same proteins indicated in (A). The major component of bovine CTP is at 18–19 kDa.

predominant proteins at about 18–23 kDa, and the quantities of these proteins were larger than that of the 16 kDa protein in human perilymph. These two antibodies also detected proteins of 63 kDa; in addition, the anti-LCCL-N antibody detected several other minor protein bands, possibly corresponding to degradation products. The anti-ivd1 (lane 3) and anti-vWF-A1 (lane 4) antibodies detected only proteins of 50–60 kDa. None of the four antibodies detected proteins of 44–40 kDa, indicating that, as in the human perilymph, there are no p44 nor p40 isoforms of Cochlin present in the bovine perilymph.

2D-GE and Western blot analysis of perilymph

To characterize further the predominant 16–23 kDa proteins detected in the perilymph with the anti-LCCL-N and anti-LCCL-C antibodies, we subjected bovine perilymph to 2D-GE analysis (Fig. 4A).

The blotted membrane was first probed with the anti-LCCL-N antibody (Fig. 4B) and the proteins were detected by chemiluminescence. The membrane was then washed, stripped, and re-probed with the anti-LCCL-C antibody (Fig. 4C). These two antibodies detected the same two lines of proteins, composed of protein spots with two different isoelectric points and different molecular weights. The more acidic isoelectric point of these proteins is 7.7; we therefore designated this group 'CTP(7.7).' The molecular weight of CTP(7.7) ranges from 18.8 to 23.1 kDa. As the more alkaline isoelectric point of these proteins is 7.9, we designated this group 'CTP(7.9).' The molecular weight of CTP(7.9) ranges from 17.7 to 22 kDa. As shown in Figs. 4B and C, the major bovine CTP component is 18–19 kDa.

Discussion

We have detected human and bovine Cochlin isoforms in the inner ear tissue and a novel Cochlin isoform in the perilymph by using isoform-specific antibodies. The positions of the peptides in Cochlin used to generate the antibodies are shown in Fig. 1B. The anti-LCCL-N and anti-LCCL-C antibodies were designed to recognize the N-terminus of only the full-length p63 isoform, the anti-ivd1 antibody was expected to detect the p63s and p44s isoforms, and the anti-vWF-A1 antibody was expected to detect all three Cochlin isoforms. As predicted, Western blot analysis using these antibodies detected one, two, and three predominant proteins, respectively, in human and bovine inner ear extracts with predicted molecular weights corresponding to the expected size of full-length Cochlin, as deduced from its cDNA and from proteomic analysis [8] (Fig. 2). We detected no other unexpected bands with these antibodies. Taken together, these data indicate that the Cochlin isoform structures are conserved in mammals and that they are consistent with our proposed domain structure of Cochlin.

The anti-LCCL-N and anti-LCCL-C antibodies detected a predominant protein of 16 and 18–23 kDa in human and bovine perilymph, respectively, in Western blots. The specificity of these antibodies indicates that the 16–23 kDa proteins correspond to the N-terminal part of full-length Cochlin as shown in Fig. 1. This molecular

weight range matches the difference between the p63 and p44 isoforms, ranging from 16 to 22 kDa as predicted from mobilities in 2D-GE [8]. We have designated this short N-terminal Cochlin isoform 'Cochlin-tomoprotein' (CTP). CTP is a novel Cochlin isoform, so far detected only in the perilymph, and thus will be an important molecule by which to understand the function of Cochlin and the pathophysiology of DFNA9 (see below). The anti-LCCL-N and anti-LCCL-C antibodies detected a single protein of 16 kDa in human perilymph; by contrast, these antibodies detected proteins of 18–23 kDa in bovine perilymph, and these were present in larger amounts than in human perilymph. The reason for this difference is not yet known; however, it is possible that the types of Cochlin isomers that are formed are species-specific.

We speculate that the N-terminal portion of full-length Cochlin is enzymatically cleaved to form the CTP isoform, which is then secreted into the perilymph. In human and bovine perilymph, all four antibodies detected proteins of 60–63 kDa, but in much small amounts as compared with CTP. One possible explanation is that these proteins are p63s and products of its degradation or processing [12,13]. The p44s and p40s were, however, not detected in the perilymph. Therefore, it seems unlikely that full-length Cochlin is processed in this compartment. Moreover, the anti-LCCL-N and anti-LCCL-C antibodies detected only p63s and not CTP in the inner ear tissue, even when coupled with chemiluminescence detection (data not shown). Taken together, these data imply that CTP is produced from full-length Cochlin by inner ear cells and then secreted into the endo- or peri-lymphatic space in the inner ear. There are other possibilities that might explain the formation of the CTP isoform; for example, the CTP isoform may be directly coded from a unique *COCH* gene splice variant or from a *COCH* homologue.

The whole molecule of CTP is composed of only an LCCL domain and to date no other proteins have been reported to have this unique character. Interestingly, all of the mutations of Cochlin reported in DFNA9 are located in CTP [7,10]. Thus, studying the role of CTP might help us to understand the function of the LCCL domain, as well as that of Cochlin. NMR structure analysis revealed that the LCCL domain adopts an unusual fold, in which a centrally located helix is wrapped by extended polypeptide segments of mostly irregular secondary structure. The N- and C-terminal ends of the LCCL domain are fairly close in space [14]. It seems likely that the function of CTP might utilize this unique structure. In the same study, Trp91 of the LCCL domain was shown to participate in interactions with a binding partner such as LPS and exhibit antimicrobial properties [14]. A previous motif analysis of the *COCH* gene has also suggested that Cochlin may have a role in host defense through antibody-independent innate immunity [9]. This hypothesis seems fairly reasonable from an anatomical point of view of the inner ear. The perilymphatic space, where CTP is found, is both connected and exposed to the outside of the inner ear labyrinth via round, oval windows, the internal auditory canal, and the cochlear aqueduct.

While this manuscript was in preparation, Robertson et al. [12] published a study of the post-translational processing of wild-type Cochlin. They used molecular biology techniques to transiently transfect the entire protein coding region of *COCH* into the mammalian cell lines COS7 and NIH3T3 cells. Expression of full-length Cochlin (HA or FLAG tagged) was detected in cell extracts by an anti-HA or anti-FLAG antibody. In the culture media, however, full-length Cochlin and only one isoform, a processed Cochlin of 50 kDa, were detected by Western blot performed after immunoprecipitation. This isoform formation pattern is very different from what we have found in human and bovine samples. Moreover, they did not detect the N-terminal fragment containing the LCCL domain (i.e., CTP) in either the cell extracts or in the culture media. This indicates that proper enzymatic cleavage and processing of Cochlin may only occur in the unique extracellular environment of the inner ear.

To date, the mechanisms of pathogenesis of the Cochlin mutations that cause the deafness disorder DFNA9 are unknown. When expressed in bacteria, most of the Cochlin mutations that cause the deafness disorder DFNA9 result in a misfolding of the LCCL domain [14]. However, expression of these mutations in mammalian cell lines did not affect the processing of Cochlin and did not cause degradation or aggregation, as is often seen in the case of misfolded proteins [12,13]. Alternatively, the pathogenesis of these mutations may stem from the complexity of Cochlin processing. By 2D-GE analysis, we detected 16 different protein spots in the bovine inner ear [8] and CTP(7.7) and CTP(7.9) in the perilymph, all of which are considered to be Cochlin isoforms. Thus, Cochlin is probably highly modified in the inner ear, and several steps of post-translational modification could account for the different molecular weight, and isoelectric points of these proteins. Such steps might include peptide bond proteolysis to remove C-terminal or other sequences for intracellular processing, action of proteolytic cascades for metabolizing secreted molecules, and chemical modifications such as glycosylation, phosphorylation, and deamination [15]. In fact, Cochlin contains two consensus sites for asparagine-linked glycosylation at residues 100 in the LCCL domain and 221 in the vWF-A1 domain [12]. When mutated, altered modification and processing of this protein and/or its interaction with the extracellular environment might lead to functional disturbance.

Elucidating the whole picture of formation and processing of the Cochlin isoforms, including the novel Cochlin isoform CTP identified here, might provide mechanistic clues to how mutations in the *COCH* gene damage the inner ear function of DFNA9 patients.

Acknowledgments

We thank Dr. James H. Shelhamer (Deputy Chief, CCMD, NIH, USA) for reviewing this paper and giving us important suggestions, especially for naming this protein as Cochlin-tomopreotein. We thank Dr. Ritsu Aoki (Deputy Head, Plastic surgery, Nippon Medical School) for advice on terminology. This study was supported by a grant for Intractable Diseases (Vestibular Disorders) from the Ministry of Health, Labour and Welfare, a grant from the Ministry of Education, Culture, Sports, Science and Technology, and a grant from the Society for Promotion of International Otorhinolaryngology (SPIO).

References

[1] W.I.M. Verhagen, S.J.H. Bom, P.L.M. Huygen, E. Fransen, G. van Camp, C.W.R.J. Cremers, Familial progressive vestibulocochlear dysfunction caused by a COCH mutation (DFNA9), Arch. Neurol. 57 (2000) 1045–1047.

[2] M. Verstreken, F. Declau, F.L. Wuyts, P.D. Haese, G. van Camp, E. Fransen, V. Hauwe, S. Buyle, R.E.M. Smets, L. Feenstra, A. van der Stappen, P.H. van de Heyning, Hereditary otovestibular dysfunction and Meniere's disease in the large Belgian family is caused by a missense mutation in the COCH gene, Otol. Neurotol. 22 (2001) 874–881.

[3] E. Fransen, M. Verstreken, W.I.M. Verhagen, F.L. Wuyts, P.L.M. Huygen, P. D'Haese, N.G. Robertson, C.C. Morton, W.T. McGuirt, R.J.H. Smith, F. Declau, P.H. van de Heyning, G. van Camp, High prevalence of symptoms of Menière's disease in three families with a mutation in the COCH gene, Hum. Mol. Genet. 8 (1999) 1425–1429.

[4] Y.J.M. de Kok, S.J.H. Bom, T.M. Brunt, M.H. Kemperman, E. van Beusekom, S.D. van der Velde-Visser, N.G. Robertson, C.C. Morton, P.L.M. Huygen, W.I.M. Verhagen, H.G. Brunner, C.W.R.J. Cremers, F.P.M. Cremers, A Pro51Ser mutation in the COCH gene is associated with late onset autosomal dominant progressive sensorineural hearing loss with vestibular defects, Hum. Mol. Genet. 8 (1999) 361–366.

[5] N.G. Robertson, L. Lu, S. Heller, S.N. Merchant, R.D. Eavey, M. McKenna, J.B. Nadol Jr., R.T. Miyamoto, F.H. Linthicum Jr., J.F. Lubianca Neto, A.J. Hudspeth, C.E. Seidman, C.C. Morton, J.G. Seidman, Mutations in a novel cochlear gene cause DFNA9, a human nonsyndromic deafness with vestibular dysfunction, Nat. Genet. 20 (1998) 299–303.

[6] E.N. Manolis, N. Yandavi, J.B. Nadol Jr., R.D. Eavey, M. McKenna, S. Rosenbaum, U. Khetarpal, C. Halpin, S.N. Merchant, G.M. Duyk, C. MacRae, C.E. Seidman, J.G. Seidman, A gene for non-syndromic autosomal dominant progressive postlingual sensorineural hearing loss maps to chromosome 14q12–13, Hum. Mol. Genet. 5 (1996) 1047–1050.

[7] S. Usami, K. Takahashi, I. Yuge, A. Ohtsuka, A. Namba, S. Abe, E. Fransen, L. Patthy, G. Otting, G. van Camp, Mutations in the COCH gene are a frequent cause of autosomal dominant progressive cochleo-vestibular dysfunction, but not of Meniere's disease, Eur. J. Hum. Genet. 11 (2003) 744–748.

[8] T. Ikezono, A. Omori, S. Ichinose, R. Pawankar, A. Watanabe, T. Yagi, Identification of the protein product of the COCH gene—hereditary deafness gene—as the major component of inner ear protein, Biochim. Biophys. Acta (Molecular Basis of Disease) 1535 (2001) 258–265.

[9] M. Trexler, L. Banyai, L. Patthy, The LCCL module, Eur. J. Biochem. 267 (2000) 5751–5757.

[10] Online Mendelian Inheritance in Man. OMIM Number: 603196.

[11] N.G. Robertson, A.B. Skvorak, Y. Yin, S. Weremowicz, K.R. Johnson, K.A. Kovatch, J.F. Battey, F.R. Bieber, C.C. Morton, Mapping and characterization of a novel cochlear gene in human and in mouse: a positional candidate gene for a deafness disorder, DFNA9, Genomics 46 (1997) 345–354.

[12] N.G. Robertson, S.A. Hamaker, v. Patriub, J.C. Aster, C.C. Morton, Subcellular localisation, secretion, and post-translational processing of normal cochlin, and of mutants causing the sensorineural deafness and vestibular disorder, DFNA9, J. Med. Genet. 40 (2003) 479–486.

[13] R. Grabski, T. Szul, T. Sasaki, R. Timpl, R. Mayne, B. Hicks, E. Sztul, Mutations in COCH that result in non-syndromic autosomal dominant deafness (DFNA9) affect matrix deposition of cochlin, Hum. Genet. 113 (5) (2003) 406–416.

[14] E. Liepinsh, M. Trexler, A. Kaikkonen, J. Weigelt, L. Banyai, L. Patthy, G. Otting, NMR structure of the LCCL domain and implications for DFNA9 deafness disorder, EMBO J. 20 (2001) 5347–5353.

[15] E. Gianazza, Isoelectric focusing as a tool for the investigation of post-translational processing and chemical modifications of proteins, J. Chromatogr. A 23 (1995) 67–87.

耳喉頭頸 76(12)：838-849，2004

Current Article

内耳プロテオーム解析と COCH 遺伝子アイソフォーム —基礎研究の臨床応用をめざして—

池園哲郎*

I. プロテオーム解析とは

ヒトゲノムの配列の解読がほぼ終了し，今後の研究の興味はゲノムから得られる情報を使い，それの意味を知ることに変わりつつある。ゲノム解析の結果，ヒト遺伝子の数は以前予想されていた10万個ではなく，それよりかなり少ない3.5万個程度であることが明らかになった。この遺伝子の数は，ヒトという生物の機能の多様性を説明するには少な過ぎると考えられている。このギャップは遺伝子が転写，翻訳される際の多様性にあることが推測されており，これを解明する手段として注目されているのがプロテオーム解析である。この概念は1996年にオーストラリアのWilkinsら[1]によって提唱された。

プロテオーム（proteome）は，細胞や組織において発現している蛋白質の全体像を指す。DNAに書き込まれた情報はRNAを介して蛋白質へ翻訳される。近年の研究によると，RNAの発現プロファイルと蛋白質の発現プロファイルは必ずしも一致するわけではなく，その相関は50%以下であるともいわれている。そこで，蛋白質の網羅的解析，すなわちプロテオーム解析を行うことが重要とされている（表1）。

一般に蛋白はDNAと比較すると取り扱いが煩雑で難しいとされている。例えば，DNAやRNAはPCRなどで増幅することが可能であるのに対し，蛋白質は増幅する技術が確立されていない。しかし，あえて蛋白の解析を行うのはなぜであろうか。その理由としてまず挙げられるのは，「ほとんどの場合，蛋白レベルでの問題が疾患を発症させる」ことにある。つまり，遺伝子レベルでの突然変異が病的蛋白を作り，酵素活性の欠如，病的蛋白の異常産生，機能喪失をもたらす。このため，生命現象に直接影響を及ぼす蛋白質を直接みることが必要で，将来的に治療を目的とする研究を行う場合は蛋白レベルでの研究が不可欠となる[1,2]。蛋白の研究はまだまだ難しい問題を抱えているが，逆にいえば今後の大きな発展が望める分野といえる。

表1 セントラルドグマとその網羅的解析

DNA	genome 解析
↓	
RNA	transcriptome 解析
↓	
蛋白	proteome 解析

プロテオーム解析の具体的方法は（1）蛋白質の分離，(2) 蛋白質の同定の2つの作業から成る。現在，もっぱら行われているのは二次元電気泳動によって蛋白質を分離し，その配列分析で目的の蛋白質を同定する方法である。蛋白質同定法には，エドマン分解を用いた蛋白質の一次配列の決定，または質量分析法がある。

内耳蛋白解析の分野ではThalmannら[3]がパイオニアであり，既に1990年に二次元電気泳動法を用いて内耳組織蛋白の解析を行い，organ of corti protein 1，2などの蛋白を同定した。しかし，

* 日本医科大学耳鼻咽喉科学教室（〒113-8603 東京都文京区千駄木1-1-5）

0914-3491/04/¥500/論文/JCLS

当時は蛋白同定に関わるデーターベースは現在のように充実しておらず，その後の大きな発展はみられなかった。その後，電気泳動関連の技術的な進歩により，現在では再現性の高い，正確な泳動結果が安定して得られるようになりつつある。

今回われわれは，二次元電気泳動による蛋白の分離後，精度が最も高いとされるエドマン分解法による配列分析を行い DNA 蛋白データーベースを用いて内耳プロテオーム解析を行った[4]。

II. COCH 遺伝子とは

非症候性遺伝性難聴は，先天性難聴の大多数を占めるといわれている。難聴・めまいなどの内耳障害に起因する症状以外に目立った異常所見がみられないこの種の難聴の原因遺伝子を同定するのは非常に困難であった。しかし，近年の分子生物学の発展によりここ数年間で急速に進歩し，現在 60 個以上の非症候性遺伝性難聴の遺伝子座が明らかになっており，このうちのべ 16 個の原因遺伝子が同定されている（http：//www.okayama-u.ac.jp/user/med/oto/oto/HHihome.htm)。これらの遺伝子の蛋白レベルでの研究は，これから大いに発展する余地のある分野である。

遺伝性内耳疾患の研究には大きく分けて 3 つのアプローチがある。

1. 原因遺伝子，およびその突然変異を探す

一般には遺伝性難聴を呈する大きな家系のゲノムを解析して遺伝子が同定される。日本は家系が小さいため困難が伴うが，最近は技術が進歩し日本の難聴家系からも新たな原因遺伝子同定の試みがなされている。

2. 患者ゲノムに「既知の」原因遺伝子の突然変異を探す

DNA チップや HPLC を応用した新たな技術開発が進んでおり，患者ゲノムの変異は以前に比べてより迅速に診断されるようになってきた。遺伝性内耳疾患に関する基礎的な知識を実際に臨床に生かすことが可能になってきている。

3. 原因遺伝子自体の研究

上記 1 の研究から，内耳に発現し重要な機能を担う遺伝子が数多く発見された。これらの遺伝子の中には COCH 遺伝子のようにその機能が未知の遺伝子も含まれており，内耳における全く新しい知見が得られている。難聴遺伝子の機能，病理を探ることを目的としており，最終的には治療法の開発を視野に入れている（今回のわれわれの研究はこの 3 に相当する)。

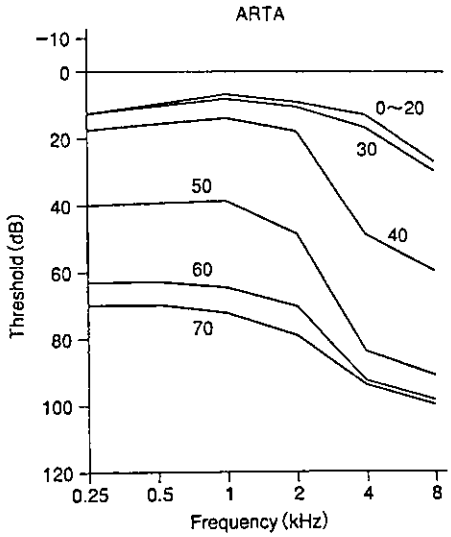

図 1 ARTA (age related typical audiogram) of DFNA9

1) DFNA9 と Cochlin について

1991 年に常染色体優性遺伝性難聴を呈する家系の内耳病理所見が Khetarpal ら[5]により報告されており，これが現在 DFNA9 と呼ばれる遺伝性難聴である。Robertson ら[6]は subtraction hybridization という手法を用いて，脳と比較してより内耳に特異的に発現する遺伝子，COCH（コークまたはコーシュ）遺伝子を同定した。COCH は 12 のエキソンから成り，クロモソーム 14（14q12-q13）に存在している。この遺伝子は，その後 1998 年に DFNA9 の原因遺伝子であることが判明した[7]。この遺伝子が作る蛋白は Cochlin（コクリン）と命名されている（通常ある遺伝子の蛋白産物には-lin が語尾に付けられる)。コクリンは内耳の細胞外マトリックス蛋白であることはわかっているが，その機能はまだ不明である。

DFNA9 はヒト病理所見，原因遺伝子，臨床所見，蛋白解析が揃って報告されている数少ない遺伝性難聴である。

その臨床像は，

①常染色体優性非症候性遺伝性難聴で 35〜55

表 2　DFNA9 mutations[9]

family	mutation		genotype
3 American families	1 missense mutation	V66G	heterozygous
	1 missense mutation	G88E	heterozygous
	1 missense mutation	W117R	heterozygous
15 Dutch/Belgian	1 missense mutation	P51S	heterozygous
1 Australian	1 missense mutation	I109N	heterozygous
1 Japanese	1 missense mutation	A119T	heterozygous
1 Hungarian	1 deletion mutation	V104	heterozygous

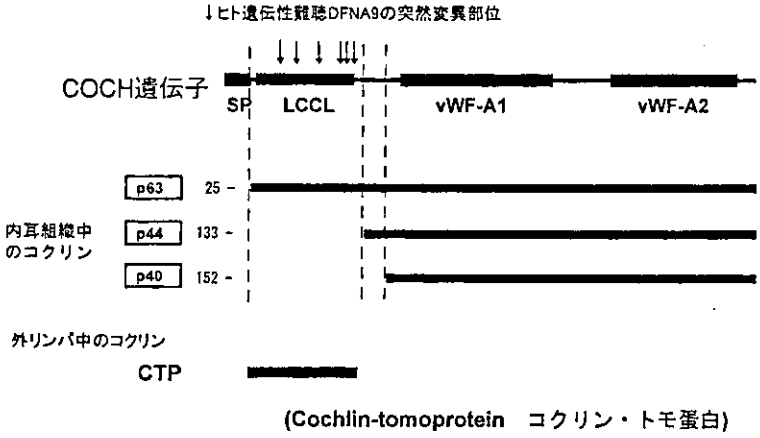

図 2　COCH 遺伝子とコクリン蛋白のアイソフォーム構造模式図
ヒト COCH 遺伝子，コクリン，ならびに今まで報告されているヒト DFNA9 の突然変異部位を示す。内耳組織中にはアイソフォーム p63，p44，p40 が発現しており，外リンパ中には CTP が発現している。突然変異は全て p63 アイソフォームの N 末端にのみ含まれており，その他のアイソフォームには含まれていなかった。

歳で発症する。

②高音が障害され徐々に中，低音域にも及ぶ感音難聴[8]（図 1）（ARTA：age related typical audiogram 参照）。

③ベルギー，オランダ，アメリカ，日本[9]，オーストラリア，ハンガリーで報告され，今まで 6 箇所の突然変異部位が報告されている（表 2）。興味深いことに，P51S の変異を呈する homozygous の患者では，より若い 25 歳で発症し，heterozygous の患者と比較して難聴の進行が速い[8]。

④耳閉感，耳鳴りを伴うめまい発作を反復する（特に PRO 51 SER タイプの症例の 25%）ことから，メニエール病との関連性が示唆されている[10]。

その病理所見では，蝸牛，前庭の広い範囲にムコポリサッカライドが沈着している。DFNA9 におけるめまい・難聴発症のメカニズムは，分子生物学的に dominant negative effect（優性ネガティブ効果）という言葉で説明されている。それは，「ヘテロ接合体において突然変異遺伝子産物がそれ自体の機能を喪失するだけでなく，正常対立遺伝子産物の機能を妨げること」を意味している。変異蛋白（ムコポリサッカライド）が内耳に沈着して機能を妨げる，もしくは変異蛋白が周囲の組織の蛋白と異常な反応を起こして異常蛋白を作る結果，神経，感覚細胞の変性をきたす，というプロセスが推察されている。

COCH 遺伝子の機能はいまだ解明されていない。一般に分子生物学では，そのアミノ酸配列のモチーフ解析から蛋白機能の手がかりを探るという手法が取られている。図 2 に示したように COCH 遺伝子には 3 つのモチーフが存在する。

(1) Signal sequence

分泌性の蛋白によくみられる配列で，その蛋白が細胞内外のどの部位に行くべきか，指令していると考えられている。

(2) LCCL module

2000年にハンガリーのグループにより命名された新しいモチーフ[11]である。下記の3つの遺伝子に含まれていることからこの名前がつけられているが，このモチーフが担う機能はまだ不明である。

①Limulus factor C：カブトガニの自然免疫能に関与，血液凝固。

②COCH：聴覚，平衡。

③LGL1：ラットの肺の発生に関与。

(3) vWF（フォンビルブランド因子）type A domain

下記に示すような多様な蛋白にみられるモチーフである。

①分泌性蛋白（可溶性，非可溶性）：止血系(vWF)，補体系（C2, factorB），免疫系（LFA-1, MAC-1etc）など。

②Extracellular matrix（CMP, Collagen 6.7.12.14)。

このモチーフにはfibrillar collagens, glycoprotein, proteoglycansへの結合作用があることが知られている。

モチーフ解析の結果と，後述するコクリン・アイソフォーム解析の結果からC末端のvWF type A domainがコラーゲンに結合し，N末端部分のLCCL moduleが何らかの重要な機能を担っているのではないかとわれわれは推測している。

後述するようにCOCH遺伝子は，①難聴，めまい両方に関与することが明らかになっている，②その発現量が内耳で非常に多い，③コクリンには等電点，分子量のheterogeneityがみられる，といった特徴をもっており，内耳の生理機能，病態解析に重要な遺伝子であることが強く示唆される。

また，コクリンは内耳特異的に多量に発現していることから，自己免疫性内耳性難聴[12]の自己抗原である可能性もある。ごく最近，細胞性免疫の観点からコクリンが自己抗原であることを示唆する報告がなされた[13]。

III. われわれの研究の結果からわかったこと

われわれは，内耳に発現する蛋白を網羅的に解析する目的で先ず研究その1（ウシ内耳蛋白の二次元電気泳動解析）を行った。その結果，コクリンに関して非常に興味深い結果が得られたため，さらに研究を発展させて研究その2（コクリン・アイソフォーム特異的抗体によるヒト内耳蛋白の解析）と研究その3（ヒト外リンパの解析による新たなアイソフォームの同定）を行った。

1. 研究その1：ウシ内耳蛋白の二次元電気泳動解析[14]

1) 方法

(1) 内耳組織の二次元電気泳動

ウシ内耳膜迷路組織を摘出しこれを20倍体積のホモジェネート液（7 M urea, 2 M thiourea, 2% Triton X100, 1% Pharmalyte, 100 mM dithiothreitol (DTT) and antiproteases mixture (Complete mini EDTA (−), Boehringer Mannheim）でホモジェネートし，蛋白を抽出する。二次元電気泳動には固定化pH勾配ゲルストリップ（Immobiline pH3-10, Amersham Pharmacia Biotech）を用いた。一次元目に尿素変性条件下で等電点泳動をMultiphor II（Amersham Pharmacia Biotech）で行い，二次元目にSDS変性下で平板ゲル（3% stacking and 12% separating polyacrylamide gel）電気泳動を行った。電気泳動ゲルを銀染色，もしくはクマシーブルーで染色した。

(2) 各スポットのアミノ酸配列を解読—遺伝子・蛋白データーベースを用いて解析—

PVDF membraneにブロットした蛋白のN末端アミノ酸配列は492 cLC pulse-liquid phase sequencer（Applied Biosystems）を用いて解読した。また，内部配列はlysylendopeptidase AP-1 (Lys-C, Wako Pure Chemical Industries）で消化したのちにペプチドをHPLC apparatus, Model 172 (Applied Biosystems）で分離し解読した。アミノ酸配列からGENETYX (Software Development) and BLAST (NCBI）などのデーターベースを用いて蛋白を同定した。